H₂ SEPARATION USING PRESSED CLINOPTILOLITE AND MIXED COPPER-CLINOPTILOLITE DISC MEMBRANES

Afrooz Farjoo, Adolfo M. Avila[†] and Steven M. Kuznicki*

Department of Chemical and Materials Engineering, University of Alberta, Edmonton, AB, T6G 2V4, Canada

Disc membranes machined from high-purity natural clinoptilolite rocks demonstrated promising hydrogen separation efficiency. However, these membranes cannot be adequately scaled up. To overcome this and provide process flexibility, mixed matrix membranes are required, pairing small particles of natural zeolite with a binder system. A novel approach was determined to use metals as binders and was tested by comparing natural clinoptilolite compact disc membranes with and without powdered copper metal. The phase composition and morphology of the discs were characterized and gas separation performance was evaluated using single gas permeation tests. Membrane selectivity for hydrogen separation was improved by applying metallic copper and copper oxide, filling a portion of the inter-particle spaces and creating adhesion with the zeolite particles.

Keywords: hydrogen separation, natural zeolites, copper, composite membranes

INTRODUCTION

Membrane technology in gas separation is becoming increasingly important in a variety of separation processes at industrial scale.[1,2] Comparing membrane separations with other separation methods such as distillation or adsorption, membranes offer a single-pass process with lower capital and operating costs, lower energy requirements, and overall ease of operation.[3,4] Membrane technology also offers promising perspectives to be integrated within sustainable energy processes.[5,6]

As the process intensification concept becomes more important, new cost-effective inorganic materials capable of being integrated into compact membrane modules are attracting both academic and industrial attention.[7,8] Inorganic zeolite membranes, as microporous poly-crystalline materials, are of particular interest due to their thermal, chemical, and acidic stability compared to polymeric or metallic membranes.[9–11]

Synthetic molecular sieve membranes for hydrogen separation have been studied in the last decades, however, their applications are limited by high production costs, technical challenges, and poor physical and chemical compatibility between thin synthetic membranes and the obligatory porous supports.[12,13] Natural zeolites, in particular clinoptilolite and chabazite, formed under high-temperature and high-pressure geological conditions, possess larger grain boundaries and demonstrate higher thermal stability than most commercial synthetic zeolites.[14–20] The small pore size coupled with the ability of the zeolite to adsorb at low partial pressures provides unique separation potential (kinetic, equilibrium, and steric) only partially fulfilled in commercially available synthetic zeolites.[16,21–23] The typical formula of clinoptilolite is $(Na^+, K^+)_6 [Al_6 Si_{30} O_{72}] \cdot _{20} H_2O$ and its framework structure contains three sets of intersecting channels of eight and ten member rings. The dimension of the largest channel of clinoptilolite framework is 0.55×0.4 nm (5.5×4.0 Å).[16,18,24] Due to the positions of the framework cations, zeolite effective pore size is smaller than most hydrocarbons and comparable with the kinetic diameter of hydrogen.[18–19,25–27]

Different inorganic composite membranes have been reported for separation of hydrogen derived from ceramics, silica, metal alloys, or zeolites widely used in gas separation.[10,28–29] Previously, we reported that natural clinoptilolite membranes directly sectioned from mineral deposits can be used for H₂ selective separation processes.[30] In order to improve the selectivity of H₂ separation, An et al.[31] used a cation exchange modification method to examine the effect of the type and size of the extra framework cations on removal of hydrogen. Dehydrogenation of light hydrocarbons is industrially important for production of chemical products.[32,33] The production yield in this reaction can be enhanced by using inorganic membranes as selective extractors of the product species. Avila et al.[34] used natural mordenite in a membrane reactor to remove hydrogen selectively and achieved an equilibrium shift in ethane dehydrogenation reaction. Shafie et al.[35] used low cost and selective natural zeolite-based cement composite membranes for H₂/CO₂ separations.

Although effective removal of hydrogen from carbon dioxide and other hydrocarbons has been achieved with these mineral membranes, scaling up to an industrial membrane technology for gas separation treatment remains a challenge. The use of mixed matrix membranes has been extensively studied in the last decades, particularly by dispersing inorganic fillers such as zeolites and carbon particles in a continuous polymer matrix. The challenge in this research area is associated with the lack of complete adhesion between the polymer phase and the inorganic particles and minimization of inter-crystalline pores correlating with poor separation performance.[36] To the best of the authors' knowledge, metals used as binders were rarely investigated. The dense structure of metals along with their malleability properties can offer clear advantages as binder materials in the preparation of inorganic mixed matrix membranes.

In this study, pressed clinoptilolite and copper-clinoptilolite composite disc membranes were prepared and tested for hydrogen separation. Copper was chosen as the binder since it is a malleable metal with high heat stability and thermal conductivity (melting point: 1085 °C) extensively used in powder metallurgical methods.[37,38]

The focus of this work is to introduce a novel approach to use natural zeolites in gas separation by applying copper metal powder as a binder material and sealant agent. Membranes were characterized using X-ray powder diffraction (XRD), scanning electron microscopy (SEM), and energy dispersive X-ray (EDX) analysis. Performance of each membrane was evaluated and compared using single gas permeation tests. Effectiveness of metallic copper was evaluated using a comparative parameter in terms of hydrogen single permeability associated with the relative average defect size of each membrane.

MATERIALS AND METHODS

Substantial differences exist in the phase purity of natural zeolite samples from various deposits. An essentially pure sample of clinoptilolite, Ash-Meadows, was provided by St. Cloud Mining Company (USA), with particle size corresponding to the 325 mesh (< 44 μm). Based on the supplier's characterization report, it is of high purity having more than 99 % clinoptilolite without any measurable levels of impurities of chabazite, quartz, or smectite. The nominal mineralogical composition of the sample was also measured and is listed in Table 1.

Copper powders were supplied by Fisher Scientific Company (Canada) with an average particle size of 25 μm and particle size distribution not larger than 63 μm.

Preparation and Characterization of Membranes

Pressed clinoptilolite discs were prepared by the dry pressing method. 3 g of zeolite powder was dry-pressed into a disc shape with a manual hydraulic press using a 19.0 mm diameter die under a pressure of 210 MPa.

To prepare mixed copper-clinoptilolite discs, metallic copper powder was added as a binding material to clinoptilolite powder to form a natural zeolite-based composite membrane. Clinoptilolite and copper powders were mixed together in a mass ratio of 1:2 (volume ratio of 2:1). Being completely mixed, the paste was dry-pressed up to 210 MPa. The resulting copper-clinoptilolite (Cu-CLI) and pressed clinoptilolite (CLI) discs had a diameter of 19 mm and thickness of 1.3 mm. They were further treated in ambient atmosphere at 650 °C for 4 h. At 650 °C, the temperature at which composite membrane discs were treated, sintering of the copper powder particles occurred. In these conditions, it was expected that metallic copper would start to diffuse across the boundaries of particles creating a complete adhesion with clinoptilolite particles and thus decreasing the effective size of inter-particle channels. After mixing with copper, sintering at high temperature, and cooling down at room temperature, the resulting discs were visually more compact and denser than the pressed CLI discs.

X-ray diffraction

To investigate the thermal stability of the membrane material, powder samples receiving thermal treatments with increasing severity were analyzed by XRD. Phase composition of composite membranes was also evaluated after applying copper and post heat treatment. XRD patterns were collected by a Rigaku Geigerflex Model 2173 diffractometer with a cobalt Co Kα radiation source ($\lambda = 1.790\ 21$ Å) run at a 2θ range of 5° to 90°.

Scanning electron microscopy (SEM)

SEM (Hitachi S-4800 FESEM) was used to characterize and observe surface morphologies of the pressed membranes.

Gas Permeation Tests

Single gas permeation of H_2, C_2H_6, and CO_2 gases supplied by Praxair Canada was used for evaluating the membrane performance in the feed pressure range of 110–160 kPa and temperature range of 25 °C to 200 °C. The gas permeation was performed using a stainless steel cross-flow membrane testing system shown in Figure 1. Membranes were sealed in a stainless steel flanged cell with graphite gaskets.

To evaluate membranes at higher temperatures, the flanged membrane cell was placed into a tubing furnace with a multipoint programmable temperature controller. A heating rate of 5 °C/min was set for each temperature interval.

Pressure was controlled by a back-pressure regulator located at the outlet of feed side. The feed and sweep gas flow rates were controlled by two mass flow controllers (Sierra Instrument Inc., Canada). For all gas permeation tests, feed and sweeping gas flow rates were set constant at 100 mL/min (STP). The retentate and permeate flow rate were measured by bubble flowmeters. An online Shimadzu Gas Chromatograph GC-14B (GC) equipped with TCD and packed column (HayeSep Q, 80–100 mesh, TCD oven = 200 °C, injector oven = 150 °C) was used to analyze the outlet gas concentrations. To achieve the maximum thermal conductivity difference between the carrier gas and the analyte, helium was used as a GC carrier gas for CO_2 and C_2H_6 while argon was used for H_2 analysis. Permeation tests at each specified temperature and pressure were repeated three times and the average number is reported in this work.

H_2, CO_2, and C_2H_6 permeances and H_2/CO_2 and H_2/C_2H_6 selectivities were calculated based on the following definitions:

$$\pi_i = \frac{N_i}{\Delta P_i} \tag{1}$$

where π_i is the permeance (mol · m^{-2} · s^{-1} · Pa^{-1}), N_i is the molar flux (mol · s^{-1} · m^{-2}), and P_a is the partial pressure difference of component i across the membrane:

$$S_{ij} = \frac{\pi_i}{\pi_j} \tag{2}$$

Table 1. EDX data for the natural clinoptilolite sample

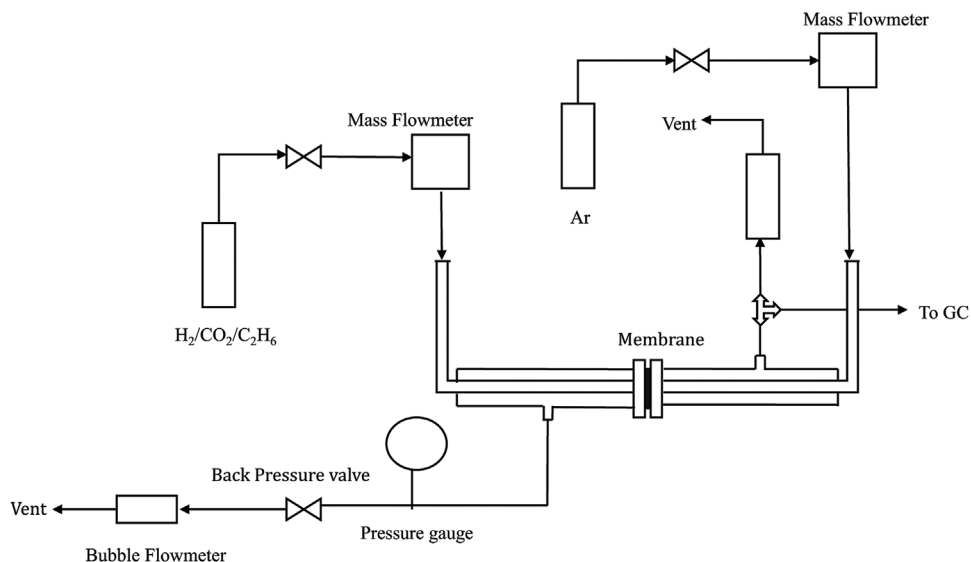|	EDX data								
	Na	K	Ca	Mg	Fe	Al	Ti	Si	Si/AL
Clinoptilolite (Atomic %)	0.553	0.361	0.047	0.063	0.0601	1	0.0036	4.124	4.125

Figure 1. Schematics of the setup for single gas permeation measurements.

where S_{ij} is the ideal selectivity of species i over j. In all the reported permeation results, there is an uncertainty estimated by a standard propagation of error analysis.[39] Absolute error propagation was the product of the uncertainties associated with different variables including pressure, temperature, flow rate, and gas chromatography measurements.

Relative Averaged Defect Size

Zeolite membranes could be screened based on the relative average defect size using a comparative coefficient obtained when H_2 single permeability is plotted as a function of pressure.[40] The H_2 permeance across the membrane can be considered as a combination of two permeance fractions. One fraction, associated with Poiseuille or viscous flow, is dependent on pressure while the other fraction is essentially not correlated with pressure variation and includes Knudsen and zeolitic flux contributions. The permeability calculated for H_2 is expressed as follows:

$$\text{Permeability } (\pi_i \delta) = \alpha_v [P^*] + \beta_{kz} \qquad (3)$$

$$P^* = P_m \frac{\Delta P}{\Delta P_i} \qquad (4)$$

The first term on the right hand side of Equation (3) is pressure dependent while the second term is invariable with pressure. P_m is the mean pressure between the feed and the permeate side. The coefficients α_v and β_{kz} are the slope and intercept of a linear fitting of the permeability data as a function of P^*. α_v is a coefficient associated with viscous flow and β_{kz} is attributed to Knudsen and zeolite fluxes. As discussed in Hejazi et al.,[40] the ratio $\lambda = \alpha_v / \beta_{kz}$ is a comparative parameter which is associated with the averaged defect size of each membrane. The membrane having the smallest averaged non-zeolite pore size corresponds to the lowest value of the $\lambda = \alpha_v / \beta_{kz}$ ratio. The values for the coefficient λ were estimated and compared for the CLI and the Cu-CLI membrane discs to evaluate the effectiveness of copper as a binder for clinoptilolite particles.

RESULTS AND DISCUSSION

XRD

Figure 2 shows the XRD patterns for clinoptilolite heat-treated at temperatures ranging from 200 °C to 900 °C. The heat-treated samples showed that increasing the temperature up to 800 °C had no significant impact on clinoptilolite crystal structure since the peak widths and locations did not change up to 800 °C. The result demonstrates the thermal stability of clinoptilolite for potential applications up to 800 °C. However the zeolite is not stable at 900 °C since the crystalline pores collapsed at this temperature.

XRD patterns of the Cu-CLI membrane heat-treated to 650 °C for 4 h are shown in Figure 3. Heat treatment in the presence of air formed CuO particles on the surface of the membranes as confirmed by XRD measurements. Sharp and high intensity peaks of the patterns are indicative of crystalline structure after copper was applied as a binder. XRD patterns also indicated that the samples were partially composed of a single phase CuO due to heat treatment while the composite membrane still maintained the crystalline structure for gas separation.
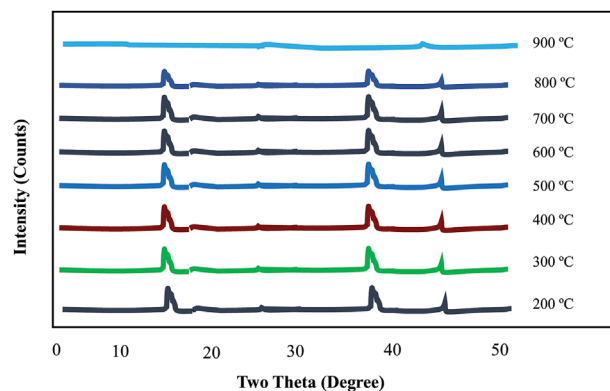

Figure 2. XRD patterns for natural clinoptilolite samples heat-treated at 200, 300, 400, 500, 600, 700, 800, and 900 °C for 1 h.
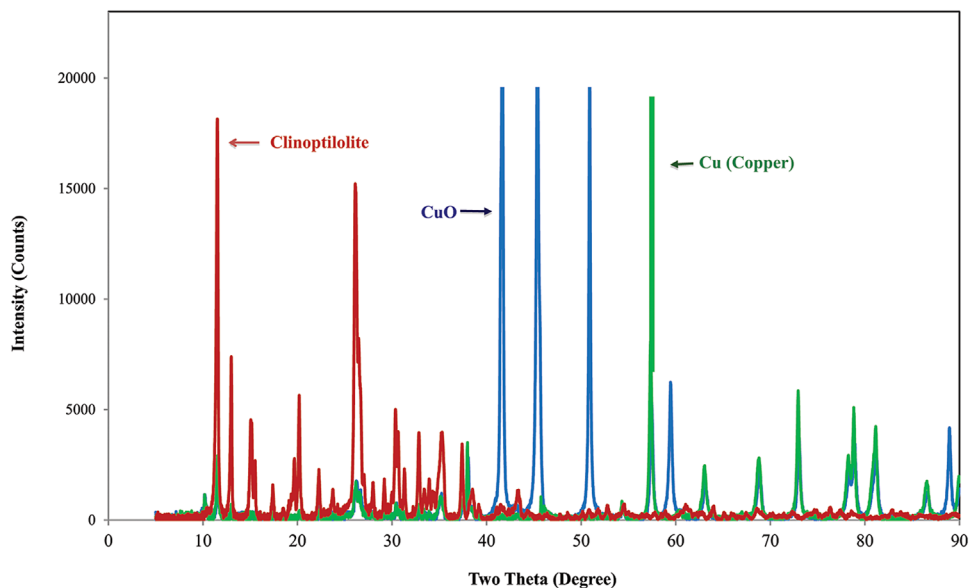
Figure 3. XRD patterns of clinoptilolite, copper, and copper oxides in Cu-CLI membrane after heat treatment up to 650 °C for 4 h.

SEM

Scanning electron and optical microscopy images of the membrane discs in ambient atmosphere are presented in Figures 4a and 4b respectively. The lighter regions on the membrane surface in Figure 4b indicate clinoptilolite material while the darker zones contain Cu° and CuO particles. Optical microscopy examination of these composite membranes also showed a dense, crack-free surface morphology and relatively uniform dispersion of CuO particles on clinoptilolite composite membrane.

Figures 4c and 4d show a schematic picture of pressed CLI and Cu-CLI composite membranes, respectively. After applying copper, a more compact matrix with a complete adhesion between particles and metal phase was obtained.

Gas Permeation Tests for Pressed Clinoptilolite Discs

Effect of temperature

Gas permeation measurement was conducted at different temperatures to determine the type of the permeation dominating in membranes. To investigate separation mechanism and membrane performance at higher temperatures, gas permeation was conducted in the range of 25 °C to 200 °C.

Figure 5 shows H_2, CO_2, and C_2H_6 permeance with molecular diameters of 0.29, 0.33, and 0.44 nm (2.9 Å, 3.3 Å, and 4.4 Å) respectively through CLI as a function of temperature.[18] The permeance of all gases, hydrogen in particular, increased slightly with the operating temperature. Since the permeance contributions associated with Knudsen and viscous flux decrease with temperature, the increasing permeation trend for all the gases with temperature reflect the larger contribution of zeolite flux at these experimental conditions.[40–45] At higher temperatures, with a weak adsorption affinity, molecules within the zeolite pores are expected to permeate based on an activated gaseous diffusion regime.[44] The combined effects of zeolitic flux behaving as an activated process and the non-zeolitic flux decreasing as temperature increases result in a modest increasing trend of the single overall permeation flux through the membranes. Then, a larger fraction of H_2 flux diffuses through the zeolite crystals
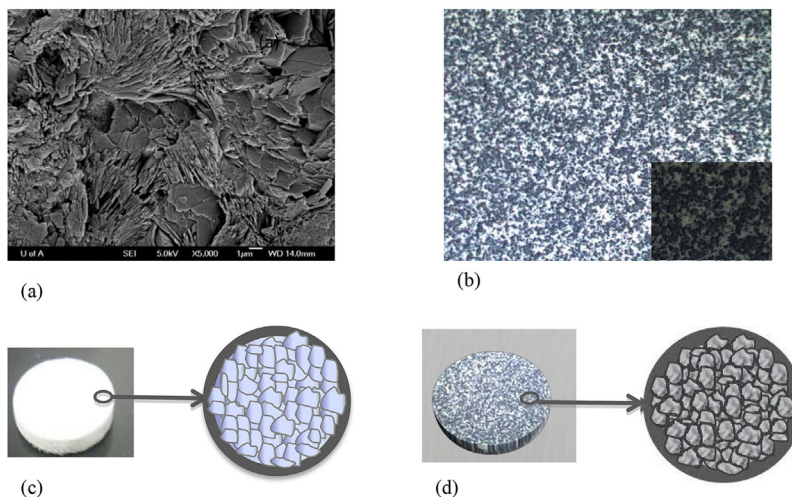

(a)

(b)

(c)

(d)

Figure 4. (a) SEM image of clinoptilolite powders, (b) optical microscopy image of Cu-CLI (16x-64X), (c) schematic of CLI membrane discs, and (d) schematic of Cu-CLI membrane discs.
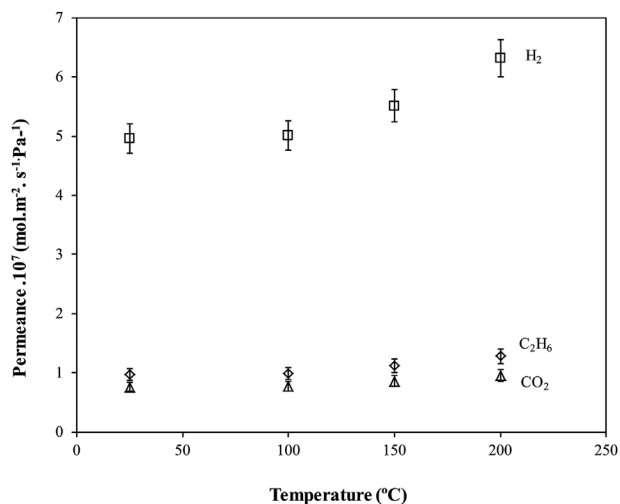
Figure 5. Single permeance of H_2, C_2H_6, and CO_2 through CLI membrane discs as a function of temperature; feed pressure: 111.2 kPa, permeate pressure: 108.0 kPa.

representing that the zeolite contribution outweighs the non-selective one and clinoptilolite particles have the potential for this type of separation.

Effect of pressure

Similar to temperature, pressure can be also used to distinguish between selective and non-selective pores in disc membranes. Pressed clinoptilolite membranes were tested at different feed pressures using H_2, CO_2, and C_2H_6 gases as well. Figure 6 shows the permeance of H_2, CO_2 and C_2H_6 at different feed pressures. Accordingly, the H_2, CO_2, and C_2H_6 permeances through the membrane discs increased, as the feed pressure was enhanced. In zeolite membranes, the permeance associated with the Knudsen flux contribution remains constant as pressure increases[40,44–46] while permeance related to the zeolitic flux is either constant for weak or non-adsorbing components (H_2) or slightly decreases with pressure for adsorbing species such as CO_2 and C_2H_6. The
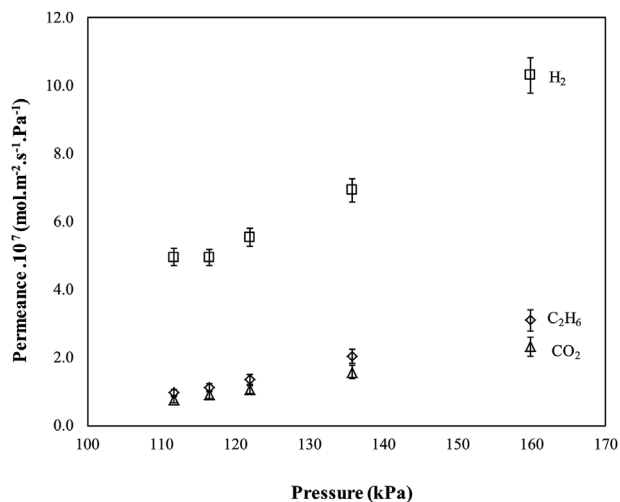

Figure 6. Single permeance of H_2, C_2H_6, and CO_2 through CLI membrane discs at different feed pressures; temperature: 25 °C, permeate pressure: 108.0 kPa.

increasing trend of permeance with pressure shows the growing viscous flux contribution through the relatively large non-zeolite pores as feed pressure increased and consequently H_2 separation efficiency decreased.[40,45,47–48]

Analogous to the permeation behaviour observed previously in natural zeolite rock discs,[30] the gas permeation across the pressed CLI discs relies on the contribution of different transport mechanisms associated with both zeolite and non-zeolite pores.

Gas Permeation Tests for Clinoptilolite-Copper Composite Membrane

In order to minimize the non-zeolite pores in the pressed clinoptilolite material discs, copper metal was mixed with clinoptilolite particles to make Cu-CLI composite membranes. Figures 7 shows the comparison for CO_2 and C_2H_6 permeances as a function of feed pressure for both types of disc membrane. Compared to CLI membranes, by applying copper as the binder, the permeation through non-selective pores for CO_2 and C_2H_6 decreased noticeably. While the CO_2 and C_2H_6 permeances for the CLI membranes increased up to 2×10^{-7} and 3×10^{-7} respectively over the pressure range of $P_{feed} = 111$–160 kPa, this value for the same gases through Cu-CLI composite membranes only reached 3×10^{-8} and 4×10^{-8} respectively representing the reduction in size and the number of non-zeolite pores after applying copper.

The CO_2 and C_2H_6 gas permeance values through Cu-CLI discs decreased significantly compared to the values obtained in the samples containing only clinoptilolite particles. CO_2 permeance across the composite membrane was only 18 % of the corresponding permeance values through the CLI discs. A similar permeance drop was also obtained for C_2H_6. Besides reducing the non-zeolite pores, a fraction of the permeance drop is associated with the reduction of zeolite content in the Cu-CLI composite material in comparison to the CLI discs. The volume fraction for the clinoptilolite content reduced when the clinoptilolite particles were mixed with copper powder. Additionally, copper and copper oxide may be also covering active zeolite pores for permeation and thus representing an additional contribution to the flux reduction. However, CO_2 and C_2H_6 gas permeance also decreased due to the non-zeolite flux reduction occurring in the Cu-CLI membranes.

Permeance rate is used to compare membranes' performance in product removal. Thus, the higher the flux, the smaller the membrane area, and the lower the capital cost of the system would be. The CLI and Cu-CLI discs provided H_2 permeance values which are comparable to those reported in the literature for micro-zeolite films supported membranes (Table 2).

Relative averaged defect size

Figure 8 shows the H_2 permeability of each membrane as a function of P^* as defined in Equation (3). Pressed zeolite (CLI) membrane showed higher permeability, as the intersection at the y-axis was larger. The corresponding values of $\lambda = \alpha_v/\beta_{kz}$ for each membrane are listed in Table 3. The CLI membrane showed a higher value of λ than the Cu-CLI membrane. This was an indication that the average defect size was smaller for the Cu-CLI composite membrane than for the CLI membrane discs. A smaller value of the average defect size represented a reduced fraction of non-zeolite fluxes for CO_2 and C_2H_6 as feed pressure increased. Therefore, the extent of the "non-selective" viscous flux passing through the relatively larger non-zeolite pores was reduced. This is consistent with a smaller defect size for Cu-CLI
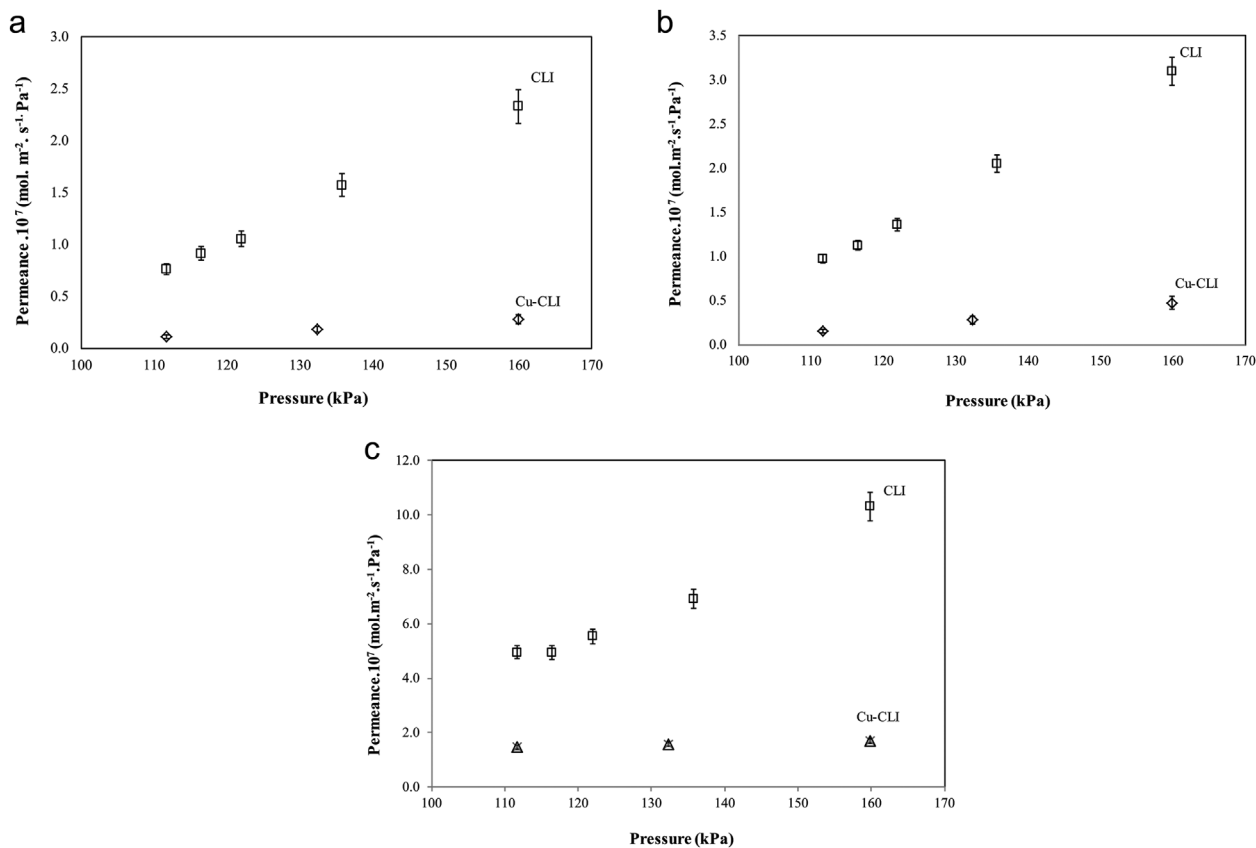
Figure 7. CO$_2$ (a), C$_2$H$_6$ (b), and H$_2$ (c) permeance through CLI and Cu-CLI membranes at different feed pressures; permeate pressure: 108.2 kPa, temperature: 25 °C.

composite as compared to the pressed CLI discs:

$$[\alpha_v / \beta_{kz}]_{Cu\text{-}CLI} < [\alpha_v / \beta_{kz}]_{CLI}$$

H$_2$ Selectivity

The selectivity values of H$_2$/CO$_2$ and H$_2$/C$_2$H$_6$ on CLI and Cu-CLI membranes are presented in Figure 9. For both membranes the H$_2$/CO$_2$ and H$_2$/C$_2$H$_6$ selectivities were higher than the corresponding Knudsen selectivity $\left(S_{H_2,CO_2}^K = \left(\frac{Mw_{CO_2}}{Mw_{H_2}}\right)^{1/2} = 4.6,\right.$

$S_{H_2,C_2H_6}^K = \left(\frac{Mw_{C_2H_6}}{Mw_{H_2}}\right)^{1/2} = 3.9\left.\right)$, which suggested that zeolite was contributing to the separation. Applying copper as a sealant and binder improved the H$_2$/C$_2$H$_6$ selectivity from 6.5 to 8 and the H$_2$/CO$_2$ selectivity from 5 to 6.2. Although the selectivity of CLI membrane was slightly higher than Knudsen, the fraction of the

Table 2. Comparison of H$_2$ permeances of different inorganic membranes

Membrane	Temperature (°C)	Permeance mol/(m^{-1} · S^{-1} · Pa^{-1})	Reference
MFI	300–500	1.2–1.8 × 10^{-7}	Caro and Noack[12]
Silicate	25–400	1.3–1.6 × 10^{-7}	Avila et al.[34]
Mordenite	25–200	1.3–1.6 × 10^{-7}	Ritter and Ebner[41]
Cu-CLI	25–200	1.1–1.4 × 10^{-7}	This work

non-selective permeance was higher than the Cu-CLI disc. However, non-zeolite regions still existed in Cu-CLI disc membranes which was confirmed by the slight increase in permeance with increasing pressure.

The increase of H$_2$ selectivity on Cu-CLI in comparison to the CLI was a clear indication that copper metal was effective as a binder for zeolite particles. H$_2$ selectivity increased because copper binder decreased the size of inter-crystalline or non-zeolite channels across the membrane disc as demonstrated with the
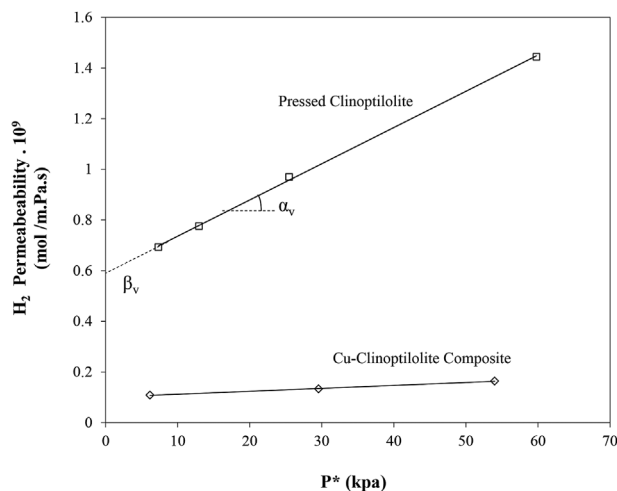

Figure 8. Comparative parameters (α_v, β_{kz}) for CLI and Cu-CLI membranes; permeate pressure: 108.2 kPa, temperature: 25 °C.

Table 3. Values of comparative parameter ($\lambda = \alpha_v/\beta_{kz}$) for CLI and Cu-CLI disc membranes

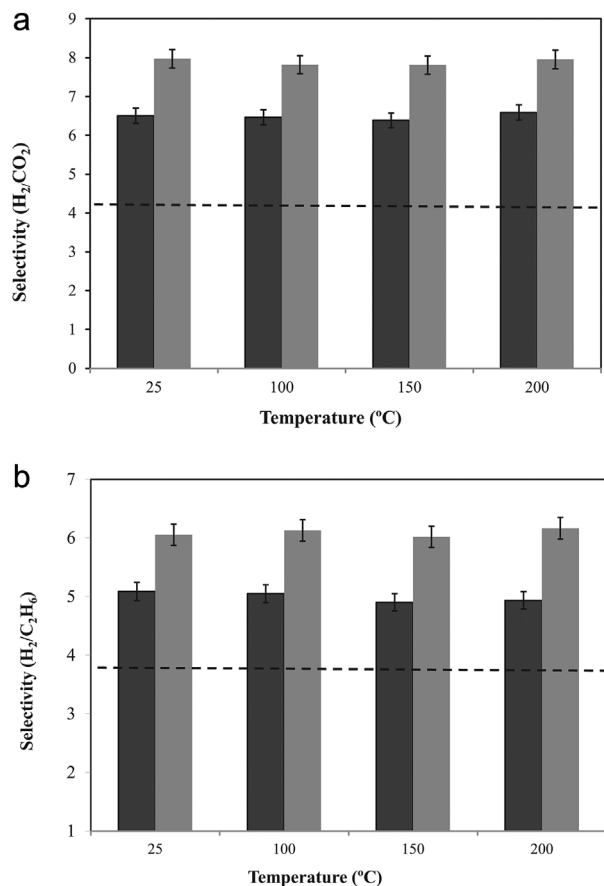| Membrane	$\lambda \times 10^3$ (kPa^{-1})
Pressed CLI	3.44
Composite Cu-CLI	1.09

Figure 9. (a) H_2/CO_2, and (b) H_2/C_2H_6 separation selectivities through CLI (black bars) and Cu-CLI (gray bars) membranes at different temperatures; feed pressure: 111.2 kPa and permeate pressure: 108.2 kPa.

estimation of the coefficient $\lambda = \alpha_v/\beta_{kz}$ shown in Table 3. Since the size of relatively large defects in the membrane decreased, the contribution of non-selective flux (viscous or Poiseuille flux) was reduced and, thus, H_2/CO_2 and H_2/C_2H_6 selectivities increased.

The copper powder made a clear improvement on the preparation of pressed clinoptilolite membrane discs. These improved characteristics of the Cu-CLI disc can be associated with the copper malleability properties and the sintering effect.

CONCLUSIONS

Zeolite molecular sieve membranes for hydrogen separation can be made from high purity and low cost natural zeolites combined with copper with bonding ability and thermal stability. Copper powders were added as binder and sealant to fill out the non-zeolite region in pressed clinoptilolite membranes. Gas permeance in copper-clinoptilolite membranes decreased due to reduction of the zeolite volume fraction and non-selective flux through inter-

particle channels. The increase of H_2/CO_2 and H_2/C_2H_6 selectivities for the copper clinoptilolite composite membranes was attributed to the metallic copper and copper oxide effectively filling a portion of the inter-particle spaces and creating a complete adhesion with the zeolite particles. The natural zeolite membrane has the additional advantage of high thermal and chemical stability, which provides the possibility of increasing the permeance at higher temperatures.

NOMENCLATURE

Mw   molecular weight (g/mol)
N molar flux (mol · s^{-1} · m^{-2})
P   pressure (kPa)
S   selectivity
t   time (s)
μ_m micron (μ)

Greek Letters

π permeance (mol · m^{-2} · s^{-1} · Pa^{-1})
δ thickness (m)

Superscript

K   Knudsen selectivity

REFERENCES

[1] J. Caro, M. Noack, P. Kolsch, R. Schafer, *Micropor. Mesopor. Mat.* 2000, *38*, 3.

[2] B. Zornoza, C. Casado, A. Navajas, *Renewable Hydrogen Technologies: Production, Purification, Storage, Applications and Safety*, Elsevier, Amesterdam 2013, p. 245.

[3] R. Abedini, A. Nezhadmoghadam, *Petroleum and Coal* 2010, *52*, 69.

[4] R. W. Baker, *Membrane technology and application*, 2nd edition, John Wiley & Sons, Hoboken 2000, p. 184.

[5] T. Tomita, K. Nakayama, H. Sakai, *Micropor. Mesopor. Mat.* 2004, *68*, 71.

[6] C. Hon, P. Li, F. Li, T. Chung, D. R. Paul, *Prog. Polym. Sci.* 2013, *38*, 740.

[7] R. T. Yang, *Adsorbents: fundamentals and applications*, John Wiley & Sons, Hoboken, 2003, p. 157.

[8] A. W. Thornton, D. Dubbeldam, M. S. Liu, B. P. Ladewig, J. Hill, M. R. Hill, *Energ. Environ. Sci.* 2012, *5*, 7637.

[9] N. W. Ockwig, T. M. Nenoff, *Chem. Rev.* 2007, *107*, 4078.

[10] M. S. Li, Z. P. Zhao, M. X. Wang, *Chem. Eng. Sci.* 2015, *122*, 53.

[11] X. Gu, Z. Tang, J. Dong, *Micropor. Mesopor. Mat.* 2008, *111*, 441.

[12] J. Caro, M. Noack, *Micropor. Mesopor. Mat.* **2008**, *115*, 215.

[13] Y. S. Lin, M. C. Duke, *Curr. Opin. Chem. Eng.* **2013**, *2*, 209.

[14] M. W. Ackley, R. F. Giese, R. T. Yang, *Zeolites* **1992**, *12*, 780.

[15] D. L. Bish, J. M. Boak, *Rev. Mineral. Geochem.* **2001**, *45*, 207.

[16] M. W. Ackley, S. U. Rege, H. Saxena, *Micropor. Mesopor. Mat.* **2003**, *61*, 25.

[17] W. An, X. Zhou, X. Liu, P. W. Chai, T. Kuznicki, S. M. Kuznicki, *J. Membrane Sci.* **2014**, *470*, 431.

[18] D. W. Breck, *Zeolite molecular sieves: structure, chemistry, and use*, John Wiley & Sons, New York **1974**.

[19] M. Nasrollahzadeh, D. Habibi, Z. Shahkarami, Y. Bayat, *Tetrahedron* **2009**, *65*, 10715.

[20] S. Wang, Y. Peng, *Chem. Eng. J.* **2010**, *156*, 11.

[21] C. Maerlocher, L. B. Mccusker, D. H. Olson, *Atlas of zeolite framework types*, Elsevier, Amsterdam **2007**, p. 156.

[22] Y. S. Lin, I. Kumakiri, B. N. Nair, H. Alsyouri, *Separ. Purif. Method.* **2002**, *31*, 229.

[23] R. Szostak, *Handbook of molecular sieves: Structures*. Springer Science & Business Media, New York **1992**, p. 119.

[24] IZA, *IZA Structure Commission*, **2002**, accessed on 16 March 2016, http://www.iza-structure.org.

[25] Y. Dond, S. Chen, X. Zhang, J. Yang, X. Liu, G. Meng, *J. Membrane Sci.* **2009**, *281*, 592.

[26] J. Dong, Y. S. Lin, M. Kanezashi, Z. Tang, *Appl. Phys.* **2013**, *104*, 121301.

[27] F. Gallucci, E. Fernandez, P. Corengia, M. V. Sint Annaland, *Chem. Eng. Sci.* **2013**, *92*, 40.

[28] N. Nishiyama, M. Yamaguchi, T. Katayama, Y. Hirota, M. Miyamoto, Y. Egashira, T. Satoh, *J. Membrane Sci.* **2007**, *306*, 349.

[29] S. Battersby, T. Tasaki, S. Smart, B. Ladewig, S. Liu, M. C. Duke, J. C. Diniz, *J. Membrane Sci.* **2009**, *329*, 91.

[30] W. An, P. Swenson, L. Wu, T. Waller, A. Ku, S. M. Kuznicki, *J. Membrane Sci.* **2011**, *369*, 414.

[31] W. An, P. Swenson, A. Gupta, L. Wu, T. M. Kuznicki, S. M. Kuznicki, *J. Membrane Sci.* **2013**, *443*, 25.

[32] T. F. Narbeshuber, H. Vinek, J. A. Lercher, *J. Catal.* **1995**, *157*, 388.

[33] A. Farjoo, F. Khorasheh, S. Niknaddaf, M. Soltani, *Sci. Iran.* **2011**, *18*, 458.

[34] A. M. Avila, Z. Yu, S. Fazli, J. A. Sawada, S. M. Kuznicki, *Micropor. Mesopor. Mat.* **2014**, *190*, 301.

[35] A. H. Shafie, W. An, S. A. Hosseinzadeh Hejazi, J. Sawada, S. M. Kuznicki, *Sep. Purif. Technol.* **2012**, *88*, 24.

[36] R. D. Noble, *J. Membrane Sci.* **2011**, *378*, 393.

[37] A. M. Abyzov, S. V. Kidalov, F. M. Shakhov, *J. Mater. Sci.* **2011**, *46*, 1424.

[38] C. Joyce, L. Trahey, S. A. Bauer, F. Dogan, J. T. Vaughey, *J. Electrochem. Soc.* **2012**, *15*, 909.

[39] P. R. Bevington, D. K. Robinson, *Data reduction and error analysis for the physical sciences*, McGraw-Hill, New York **1992**, p. 1.

[40] S. A. H. Hejazi, A. M. Avila, T. M. Kuznicki, A. Weizhu, S. M. Kuznicki, *Ind. Eng. Chem. Res.* **2011**, *50*, 12717.

[41] J. A. Ritter, A. D. Ebner, *Separ. Sci. Technol.* **2007**, *42*, 1123.

[42] A. M. Tarditi, E. A. Lombardo, A. M. Avila, *Ind. Eng. Chem. Res.* **2008**, *47*, 2377.

[43] R. M. Barrer, *J. Chem. Soc.* **1990**, *86*, 1123.

[44] M. Kanezashi, Y. S. Lin, *J. Phys. Chem. C* **2009**, *9*, 3767.

[45] E. A. Mason, A. P. Malinauskas, *Gas transport in porous media: The dusty-gas model*, Elsevier, Amsterdam **1993**, p. 142.

[46] H. Li, R. Dittmeyer, *Chem. Eng. Sci.* **2015**, *127*, 401.

[47] S. Colin, *Microfluid. Nanofluid.* **2005**, *1*, 268.

[48] S. Thomas, R. Schäfer, J. Caro, A. Seidel-Morgenstern, *Catal. Today* **2001**, *67*, 205.